Bayesian Decomposition of Surface EMG

Kevin R. Wheeler[*]
Computational Sciences Division
NASA Ames Research Center
Moffett Field, CA 95033

Mindy Chang
EE & CS Dept.
MIT
Cambridge, MA 02139

Kevin H. Knuth
Computational Sciences Division
NASA Ames Research Center
Moffett Field, CA 95033

Abstract

This paper presents a Bayesian algorithm to separate surface Electromyograms (EMG) into representative motor unit action potentials. The algorithm is based upon differential Variable Component Analysis (dVCA) [1, 2] which was originally developed for Electroencephalograms. The algorithm uses a simple forward model representing a mixture of motor unit action potentials as seen across multiple channels. The parameters of this model are iteratively optimized in turn for each component. Results are presented on both synthetic and real EMG data. The synthetic case has additive white noise and is compared with known components. The real EMG data was obtained using a custom linear electrode array designed for this study.

1 INTRODUCTION

We present a Bayesian method to perform source separation for surface Electromyograms (SEMG). In particular, compound motor unit action potentials (CMAPs) [3] are separated into representative motor unit action potential (MUAP) waveforms. Our method is based upon the differentially Variable Component Analysis algorithm (dVCA) for source separation of Electroencephalograms (EEG) developed by Knuth et. al. 2004 [1, 2]. We have extensively modified this algorithm to work with SEMG.

Electromyograms are used in the medical community to aid in diagnosis of neuro-muscular diseases, to interface with prosthetics, and as a means to interface with virtual devices [4]. Voluntary limb movement occurs as a result of the brain generating a spike train that is transmitted through the nerve to a junction in the muscle known as the end-plate region. This induces an ion transfer along the length of the muscle fibers with a corresponding contraction of the muscles. The traveling waveform along the muscle fiber is known as a motor unit action potential. This ion exchange induces a current on the surface of the skin which can be measured as a voltage via a resistive electrode. For precise clinical applications it is often necessary to use invasive needle electrodes to try to measure individual motor unit action potentials. On the surface of the skin many MUAPs are mixed together and are measured as surface EMG.

For long duration studies and applications, non-invasive methods are less prone to the complications that can arise with needle and device insertion. Unfortunately, noninvasive methods result in greater signal complexity due to multiple MUAP sources being mixed as they traverse through skin, fat, muscle and other tissues. In this paper, we concentrate on a Bayesian approach to solving this mixing problem. There has been extensive research on decomposing EMG [5, 6, 7, 8] using non-Bayesian approaches.

In any standard Bayesian methodology, it is necessary to have a forward model and a means to optimize the parameterization of that model based upon data observations. In the case of EMG, we have chosen to develop a model that describes the MUAPs and how they are mixed together. There has been great progress made [9, 10, 11, 12, 13] in developing physics-based forward models for EMG signal generation as measured on the surface of the skin. Unfortunately, in most of this literature, there is a gap between the methods of decomposition and model parameterization that could be bridged by following a Bayesian approach. In this paper, we detail the steps that we have taken to fill this gap with a simple mixing model.

The *METHOD* section describes the Bayesian decomposition algorithm, the synthetic data simulations, and the experiment design for obtaining subject EMG. The results of applying our decomposition algorithm to both the simulated data and the real data are presented in the *RESULTS* section.

Corresponding author: kwheeler@mail.arc.nasa.gov

2 METHOD

The model that we formulate for separating mixed MUAPs is dependent upon how we acquire the data. Ideally, within a Bayesian framework we would model every part of the system. We would start by modeling the sources of the potentials; how the shape of the potentials is changed by transmission through the tissue. This would be followed by a model of the electrodes, the amplifier, and finally of the data acquisition card. The model we present relies on approximations to reduce the task of modelling all of these elements. Before going into detail on the model, it is necessary to define the data collection technique.

2.1 Experimental Design

Our model is based upon the assumption that we can observe compound MUAPs along parallel fibers of a muscle group. This assumption is supported by using a linear electrode array [14] [9] as shown in Figure 1. We fabricated this electrode array with parallel silver bars spaced 5 mm apart. Figure 2 shows the data collected by this device on four channels. Note that a star has been placed over one of the action potential waveforms which is shifted between channels proportional to the conduction velocity. The muscle contraction under study is assumed to be constant. The contraction level in this work is approximately 20 percent of maximum voluntary contraction.
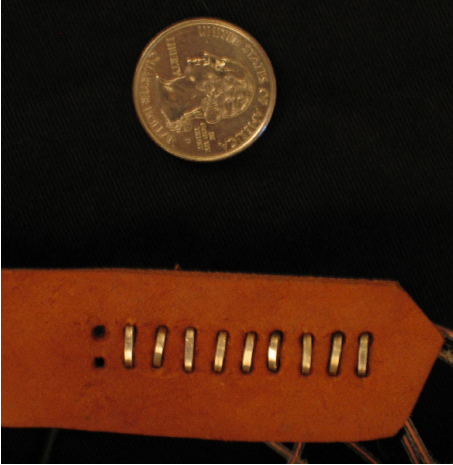

Figure 1: Linear electrode array pictured with a U.S. quarter.

2.2 Model

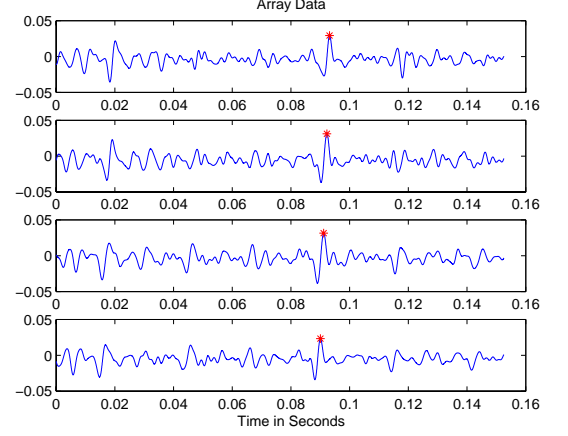Our model representing the mixing process for the mth channel as a function of time can be expressed as:

Figure 2: EMG data from linear electrode array. Star indicates moving MUAP over time between channels.

$$
\begin{aligned}
\psi_{m,t} = & \sum_{n=1}^{N} \sum_{f=1}^{F} C_{mn} \alpha_{nf} s_n(t - (m - m_{ref})\tau_n^C \\
& - (f-1)\tau_n^F - \tau_{nf}^S)
\end{aligned} \tag{1}
$$

where N is the number of sources (components), F the number of firings, C represents the coupling between channels and sources, $s_n()$ is the source waveform, α_{nf} is the amplitude weighting. τ_n^F represents the time delay associated with the firing frequency of a particular source, τ_n^C is the delay across channels which is proportional to the conduction velocity, τ_{nf}^S is the latency for each source and firing representing the variability in firing.

There are several assumptions that underlye (1). We assume that the electrode array is positioned parallel to the muscle fibers and that the electrodes are evenly spaced apart. These assumptions allows us to know that as the dominant components travel along the muscle fibers, that they move from channel to channel. The time it takes to go from one channel to the next is represented by τ_n^C. We also assume that the muscle contraction is of constant force and that the sampling time is short enough to assume that the firing rate (or time delay between firings τ_n^F) of any one MUAP source is constant. The variation in the periodicity of the firing of a single source is modelled by τ_{nf}^S and is assumed small with respect to the firing rate.

The basis of model parameter estimation lies in using Bayes' Theorem to maximize the probability of the model, using the likelihood of the data and the prior probability of the model parameters and other known information (symbolized by I):

$$
p(model|data, I) = \frac{p(data|model, I)p(model|I)}{p(data|I)} \tag{2}
$$

Substituting the parameters of our model, this becomes

$$P = p(C, s(t), \alpha, \tau^F, \tau^C, \tau^S | x(t), I) =$$

$$\frac{p(x(t)|C, s(t), \alpha, \tau^F, \tau^C, \tau^S, I)p(C, s(t), \alpha, \tau^F, \tau^C, \tau^S | I)}{p(x(t)|I)}$$

where the value on the left-hand side of the equation, which will be referred to as P, is the posterior probability of a model describing the data. The right side represents the product of the likelihood of data given the model and the prior probability of the model, divided by a proportionality constant dependent on the data. A uniform distribution is assigned to the prior probabilities of each parameter, and as a result the posterior probability P becomes directly proportional to the likelihood of the data:

$$P \propto p(x(t)|C, s(t), \alpha, \tau^F, \tau^C, \tau^S, I) \quad (3)$$

Using the principle of maximum entropy, the likelihood of the data is assigned a Gaussian distribution by introducing a new parameter σ. This parameter represents the expected squared error in prediction and is assigned a Jeffreys prior for maximum uncertainty. When the likelihood is marginalized over all values of σ, the result becomes

$$P \propto (2\pi\sigma^2)^{-\frac{MT}{2}} Exp\left[-\frac{1}{2\sigma^2}Q \right] \quad (4)$$

where Q represents the square of the residuals between the data and our model, summed over all time points in all channels

$$Q = \sum_{m=1}^{M} \sum_{t=1}^{T} \left(x_m(t) - \sum_{n=1}^{N} \sum_{f=1}^{F} C_{mn} \right.$$
$$\alpha_{nf} s_n(t - (m - m_{ref})\tau_n^C$$
$$\left. -(f-1)\tau_n^F - \tau_{nf}^S) \right)^2$$

To simplify calculations we maximize P by maximizing the log of P. Using the method described by Knuth, et al. [1, 2], the log of the posterior probability P can be written as:

$$lnP = -\frac{MT}{2}lnQ + const \quad (5)$$

For convenience of discussion, two commonly used expressions in the process of minimizing the difference between the data and the model, are defined below. For a given component j in channel m at time t, U represents all firings of the component j deduced from the value of all other pa-

rameterized components subtracted from the actual data.

$$U(j, m, t) = x_m(t) - \sum_{\substack{n=1 \\ n \neq j}}^{N} \sum_{f=1}^{F} C_{mn}$$
$$\alpha_{nf} s_n(t - (m - m_{ref})\tau_n^C$$
$$-(f-1)\tau_n^F - \tau_{nf}^S) \quad (6)$$

Similarly, the expression U_F isolates a particular firing, f_0 of the jth component in channel m at time t, using the same method of deduction by also subtracting away all other firings of the jth component except for the f_0^{th} firing.

$$U_F(j, f_0, m, t) = U(j, m, t) - \sum_{\substack{f=1 \\ f \neq f_0}}^{F} C_{mn}$$
$$\alpha_{nf} s_n(t - (m - m_{ref})\tau_n^C - (f-1)\tau_n^F - \tau_{nf}^S) \quad (7)$$

2.2.1 Waveshape

The Maximum A Posteriori estimate of the waveshape is found by setting the partial derivative of the log probability with respect to a time point q in waveshape s_j to zero. Details appear in Knuth 2004 [1].

2.2.2 Amplitude

When taking the partial derivative of the log probability with respect to the amplitude of the f_0^{th} firing of the jth component, the optimal estimate for the amplitude of this particular firing becomes

$$\hat{\alpha}_{jf_0} = \frac{\sum_{m=1}^{M} \sum_{t=1}^{T} U_F R_\alpha}{\sum_{m=1}^{M} \sum_{t=1}^{T} (R_\alpha)^2} \quad (8)$$

where

$$R_\alpha = C_{mj} s_j(t - (m - m_{ref})\tau_j^C - (f_0 - 1)\tau_j^F - \tau_{jf_0}^S) \quad (9)$$

Since the model allows for varying amplitudes between different firings of the same component, each α_{jf} term is determined irrespective of other firings by using the deduced single firing term, U_F.

2.2.3 Firing Period

To find the optimal estimate for the firing period of the jth component,

$$\hat{\tau}_j^F = argmax \, Y(\tau_j^F) \quad (10)$$

here

$$Y(\tau_j^F) = \sum_{m=1}^{M} \sum_{t=1}^{T} U(j, m, t)U(j, m, t + \tau_j^F) \quad (11)$$

where the function U is defined in (6). The function $Y(\tau_j^F)$ represents the autocorrelation across each channel, summed across all channels for all firings of a given component j. The jth component is isolated by subtracting away all firings of all other components as shown in equation to obtain $U(j, m, t)$. Each channel is multiplied with shifted versions of itself, and assuming that the data is periodic across each channel, the latency shift that produces the maximal value will be where the 2nd through F^{th} channel is closest to alignment with the 1st through $(F-1)^{st}$ firing of the jth component. This latency estimate is constrained to be positive and greater than 2 ms because a firing period that is significantly smaller than the time span of a single action potential is not physiologically plausible.

2.2.4 Conduction Period

To find the optimal estimate for the conducting period of the jth component,

$$\hat{\tau}_j^C = argmax\, Z(\tau_j^C) \tag{12}$$

where

$$Z(\tau_j^C) = \sum_{m=1}^{M} \sum_{t=1}^{T} U(j, m-1, t) U(j, m, t + \tau_j^C) \tag{13}$$

where the function U is defined in equation 6. The function $Z(\tau_j^C)$ represents the cross-correlation between consecutive channels, summed across all pairs of channels for a given component j. As above, the estimate of the jth component (with all of its firings) is obtained by subtracting away all firings of all other components to obtain $U(j, m, t)$. As a convention, the first channel will be considered the reference electrode from which action potentials are first detected. As action potentials propagate through the muscle fibers, each subsequent channel detects the action potential slightly later than the previous channel. For each pair of channels, the first channel is multiplied with shifted versions of the second channel. Assuming that the data is periodic across each channel, the latency shift between channels that produces the maximal value will be where all firings of the jth component most nearly align between the pair of channels. The conduction period is constrained to positive values between zero and half of the firing period. Since the conduction period is significantly smaller than the firing period, we are able to use this assumption.

2.2.5 Offset Latency

To find the optimal estimate for the offset latency of f_0^{th} firing of the jth component,

$$\hat{\tau}_{jf_0}^S = argmax\, A(\tau_{jf_0}^S) \tag{14}$$

where

$$A(\tau_{jf_0}^S) = \sum_{m=1}^{M} \sum_{t=1}^{T} U_F(j, f_0, m, t) V_F(j, f_0, m, t + \tau_{jf_0}^S) \tag{15}$$

where the function U_F and $V_F(j, f_0, m, t)$ represents the reconstruction of the f_0^{th} firing of the jth component, using all other parameters of the jth component

$$V_F(j, f_0, m, t) =$$

$$C_{mj}\alpha_{jf_0} s_j(t - (m - m_{ref})\tau_j^C - (f_0 - 1)\tau_j^F - \tau_{jf_0}^S)$$

The function $A(\tau_{jf_0}^S)$ represents the cross-correlation between the deduced single firing of the jth component, $U_F(j, f_0, m, t)$, based on the data after removing the firings of the other components, and the estimated single firing of the component, $V_F(j, f_0, m, t)$, based on the jth component parameters. The deduced firing is multiplied with shifted versions of the reconstructed firing, and the latency which produces the maximal value is taken as the estimate of the offset latency.

2.2.6 Adjustment for Latency Degeneracy

Since τ_n^F and τ_{nf}^S both represent time shifts with respect to a single channel of data, if the estimated value for τ_n^F is inaccurate to begin with, τ_{nf}^S values will linearly increase in amplitude. For example, if the estimated τ_n^F value is smaller than the actual value, each successive firing will deviate from its estimate by a larger value than the previous firing with its respective estimate. For a given firing f of a given component n, the value of the total latency due to firing and offset is not affected, but τ_n^F and τ_{nf}^S values no longer represent the firing period and offset period. In order to correct this, every time the τ_{nf}^S is calculated, a linear regression on the τ_{nf}^S values is performed and both latency values are adjusted accordingly. The linear regression takes the form of $\tau_{nf}^S = \mu_n \cdot f + \beta_n$ Using this line, τ_n^F and τ_{nf}^S values are remapped so that τ_{nf}^S becomes a constant value plus or minus deviations from the regression line, d_{nf}, and τ_n^F accounts for this change.

$$(f - 1) \cdot \tau_j^F + \tau_{nf}^S =$$

$$(f - 1)\tau_n^F + (\mu_n f + \beta_n + d_{nf}) =$$

$$(f - 1)\tau_n^F + (\mu_n(f - 1) + \mu_n + \beta_n + d_{nf})$$

$$= (f - 1)(\tau_n^F + \mu_n) + (\mu_n + \beta_n + d_{nf})$$

The adjusted τ_j^F value becomes

$$\bar{\tau}_j^F = \tau_j^F + \mu_n \tag{16}$$

and the τ_{nf}^S value becomes

$$
\begin{aligned}
\bar{\bar{\tau}}_{nf}^S &= \mu_n + \beta_n + d_{nf} \\
&= \mu_n f + \mu_n + d_{nf} - (f-1)\mu_n \\
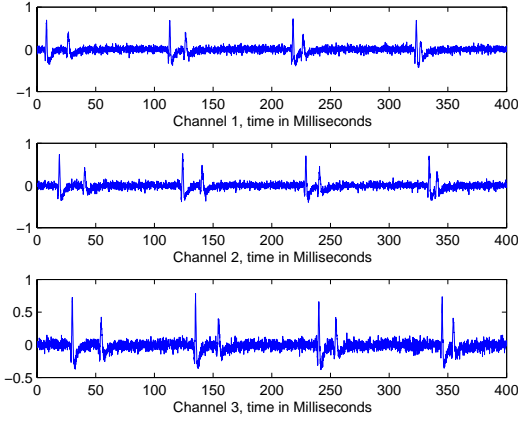&= \tau_{nf}^S - (f-1)\mu_n
\end{aligned}
\qquad (17)
$$

Figure 3: Compound motor unit action potentials with white noise.

2.2.7 Iterations

The order in which the parameters are optimized can be altered with varying effects, but the structure used for this paper is as follows:

1. Identify the total number of firings within the dataset by human observation.

2. Estimate τ_n^F for the component using (10), (11).

3. Estimate τ_n^C using (12), (13).

4. Estimate τ_{nf}^S using (14), (15).

5. Adjust τ_n^F values if τ_{nf}^S values show a linear rate of change using (16),(17).

6. Estimate the waveshape $s()$

7. Estimate the amplitude α of each firing using (8).

8. To parameterize another component, follow steps 1-5, using the data from which the model of the first component has been subtracted.

9. Iterate through steps 1-5 for both components until the average change in waveshapes from the previous iteration is less than 1% or until a maximum number of iterations has been performed, and align the peaks of the component waveshapes, adjusting τ_{nf}^S accordingly.

10. For each additional source, parameterize the new component based on the data without all other components that are already modeled, and repeat the iteration of steps 1-5 for all components until a stopping condition in step 9 is reached.

Initialization Since the general waveshape of a MUAP is fairly well-defined, this information is used to initiate the waveshape. The point values in s(t) are determined in the manner described below in the Synthetic Data section. As mentioned earlier, the coupling matrix is set to all ones under the assumption that all detectors receive signals from all components equally well. All latency values, τ_n^F, τ_n^C, and τ_{nf}^S are initialized as zero, and all α_{nf} values are one. Since the latency optimizations occur first in the iteration in steps 2-4, α_{nf} values are initialized as one. If the α_{nf} values were zero, the reconstructed component used in the τ_{nf}^S calculation would just be a straight line at zero. For this reason, if any value of α_{nf} becomes zero in the process of iteration, the α_{nf} value is set to one temporarily for the calculations of τ_n^F, τ_n^C, and τ_{nf}^S and then set back to zero.

Estimating τ_j^F and τ_j^C before τ_{jf}^S When considering a single component, τ_j^F and τ_j^C are parameters that characterize the component, providing information about the firing rate and conduction velocity when the distance between electrodes is known. The optimization of τ_j^F and τ_j^C involve correlations of the deduced component and are not directly dependent upon the accuracy of the parameters of the component in question. On the other hand, τ_{jf}^S "picks up the slack" in the overall latency value and is restrained to be a constant with slight deviations for each firing. Effectively, this constant gives information about the relative offset between different components, and the deviation represents the time error between the model and actual data for each firing of this particular component. τ_{jf}^F involves the cross-correlation of the deduced component and the reconstructed component and therefore is directly dependent upon the accuracy of the jth component parameters.

In determining the order of this algorithm, the τ_{jf}^S calculation is performed after τ_j^F and τ_j^C so the offset calculation has the benefit of using the already parameterized firing and conduction period values when reconstructing the jth component for cross-correlation. When the latency values are remapped in step 5, the firing period adjustment is applied to a τ_j^F value that represents an estimate of the firing period rather than an initial value with no significance.

Estimating the waveshape before amplitude Due to the degeneracy that could occur in the model between the scaling of the waveshape and the amplitude, the waveshape is constrained to have a peak-to-peak amplitude of one to give the α values a consistent meaning. Thus in each set of iterations, the waveshape is estimated first and scaled peak-to-peak. The amplitude α is parameterized after the

waveshape has been determined so that α can appropriately compensate for the waveshape scaling in each firing of the component in question.

Aligning waveshapes and adjusting τ_{nf}^S   A degeneracy also occurs in the time domain between the waveshape and the offset latency τ_{nf}^S. A time shift in the component could either be characterized as a change in waveshape or a shift in offset latency. In order to give the offset latency values a relative meaning between different components, each time a stopping condition is met, as in step 9, the peaks of all component waveshapes are aligned to match the wave-shape with the earliest peak, and each τ_{nf}^S value is adjusted accordingly. This alignment is performed after each stopping condition to ensure that the algorithm has had a chance to estimate all parameter values before shifting all wave-shapes to an earlier time. Performing the alignment during the iterative process runs the danger of shifting parts of the waveshape out of the time-frame allotted for a a single waveshape into negative time, which is invalid for this model.

Only optimizing new component on its first iteration When parameterizing a new component j, all previous components have already been optimized to their stopping condition. In all parameter optimization calculations (steps 1-5), the deduced component is used, either in the form of a single firing or an action potential train. For the first iteration, since the jth component has not yet been completely parameterized, using this component in calculations for other components may throw off parameter values unnecessarily. Therefore, for the first iteration of a new component j, all parameters of j are optimized. For successive iterations, all parameters are optimized for each component in turn.

2.3   Synthetic Data

The waveshape of the synthetic data used for testing is based on the MUAP model developed by McGill, Lateva, and Xiao 2001 [15]. The source function, $V'(t)$ was created by the sum of a scaled spike and afterpotential

$$\frac{dV(t)}{dt} = (ag'(t) + bg(t)) - \frac{b}{t_A} g(t) * \left(e^{-t/t_A} u(t) \right) \quad (18)$$

where * denotes a convolution, a and b are scaling factors, t_A is a time constant of decay, and

$$g(t) = \frac{k^{n+1}}{\Gamma(n)} t^n e^{-kt} u(t) \quad (19)$$

in which n and k are adjustable constants. The standard values used were $n = 2.5$ and k$= 5.8$ [15]. This source function was used as the initial estimate of all new component waveshapes. The model described by McGill, et al. also details spatial and temporal weighting functions

to be convolved with the source function representing the waveshape distortion as it travels along the muscle fibers, as well as considerations for different lengths of muscle fibers. These factors were not implemented for this paper, but a convolution was performed using an approximate weighting function in generating the synthetic data. For simulation, varying levels of Gaussian noise were added as well. The data shown in Figure 3 was generated with the two components shown in Figure 4, that were mixed together with uncorrelated white noise with a signal to noise ratio of 3.7. This level of noise appeared to be higher than that normally expected in an experimental setting, and thus is representative of a harder than normal test.
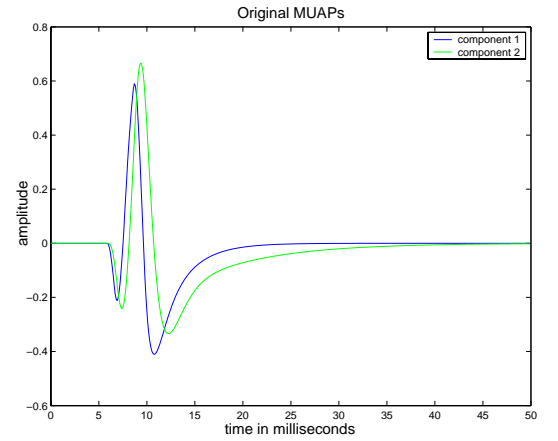

Figure 4: Synthetic motor unit action potentials

2.4   Real Data

The subject EMG data was acquired using our electrode array positioned over the bicep. The subject was required to lift and hold a 5 pound weight and was only allowed to bend at the elbow, with the elbow supported. The data was sampled at 32 kHz. using a custom built amplifier with a gain of 1000 and an anti-aliasing filter with a 3 kHz cutoff frequency.

3   RESULTS

3.1   Synthetic data

The two component synthetic data was separated using the described algorithm for 20 trials. The data consisted of three channels with only four firings across the channels. A typical decomposition is shown in Figure 5. This resulted in a median RMS error of 0.0297.

3.2   Real data

The real data, that is partially shown in Figure 6, was decomposed into two components shown in Figure 7. Since
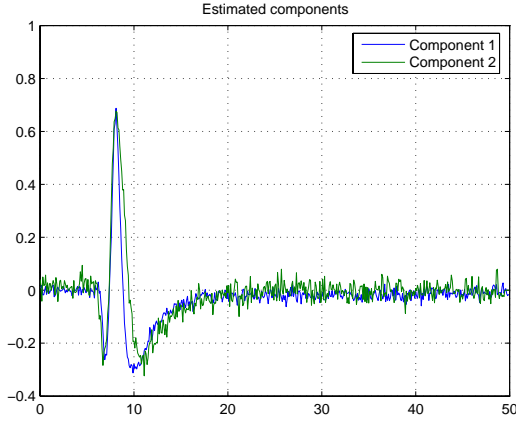
Figure 5: Recovered synthetic components

this was real data we do not have the actual MUAPs to which to compare our decomposition, so instead we compare this with a method in which clean MUAPs were hand-picked and then averaged together. This averaged MUAP waveform is depicted in Figure 8. From this, it can be seen that there is qualitative agreement between the expected MUAP and the first component discovered using this algorithm. The second component contains multiple compound MUAPs because only two components were specified to be calculated.
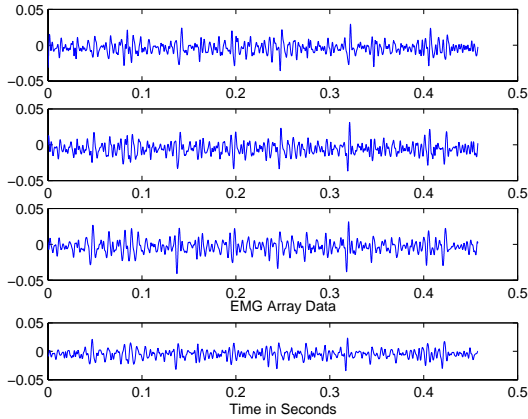

Figure 6: EMG data.

4 CONCLUSION

The original dVCA algorithm designed for EEG was substantially modified for the purpose of separating compound MUAPs measured in surface EMG. This algorithm was demonstrated on both simulated and real EMG data. The results are encouraging for both the synthetic and real cases. The most flexible part of this algorithm is in letting the waveform $s(t)$ vary over time. Letting the wave-
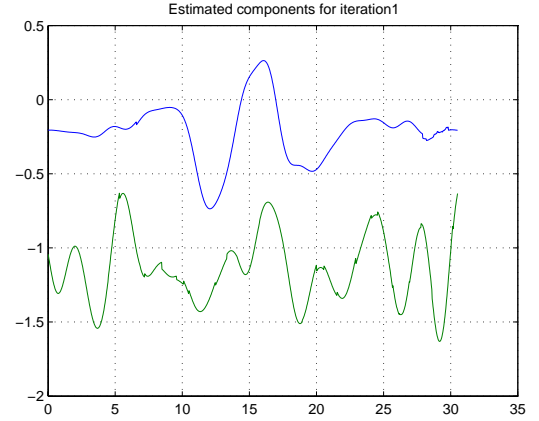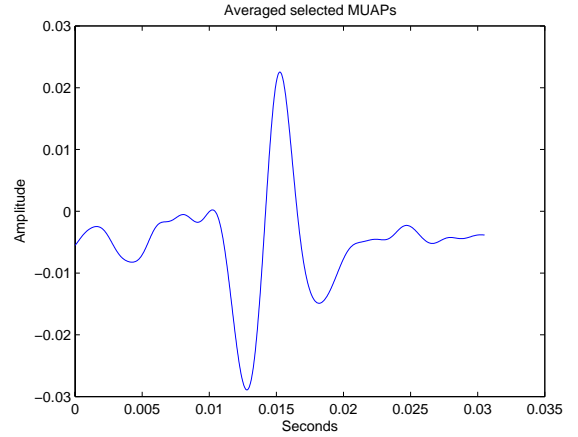

Figure 7: Both components from real data.

Figure 8: Average waveform of hand selected MUAPs.

shape be pointwise estimated allows it to have any shape, even shapes which are not at all physiologically plausible. This flexibility was deliberate to determine if the algorithm would discover waveshapes resembling expected MUAP shapes. Indeed, we were pleased to see that the discovered components do resemble the synthesized MUAPs. To this end, we have obtained MUAPs from surface electrodes that are remarkably similar to our expected waveform without imposing any knowledge of what we were expecting to see in terms of shape.

In order to improve the efficiency of the algorithm, the next generation should incorporate parameterized waveshape constraints rather than pointwise estimates since this is the most computationally expensive part of the algorithm. Such constraints could take a number of different forms. For example, we could work in the space of parameterizable functional bases (such as splines or Hermite polynomials). In this paper we have shown the decomposition into two components, but decomposing into any number of components is possible. We do not attempt to

identify the correct number of components here, details of how one might enable this algorithm to select the number of components are presented in [1].

If additional experimental trials were to be considered, it would be interesting to perform a study whereby needle electrodes were used to record the MUAPs simultaneously with surface electrodes. This would help to verify that the algorithm is able to identify individual sources. This would also give us enough data to incorporate and parameterize a detailed convolutional model of how the detected signals are distorted as they traverse through the skin.

It is our sincere hope that we have shown the utility of a Bayesian approach to modeling and decomposition of EMG data. The approach shown is a simple forward mixing model. This model could be replaced with a much more complicated physics-based model (such as the electromagnetic model of [11]). This would then allow for the automated determination of the representative tissue properties via proper model parameterization at the expense of more complex optimization.

Acknowledgements

References

[1] K.H. Knuth, A.S. Shah, W.A. Truccolo, S.L. Bressler, M. Ding, and C.E. Schroeder. Differentially variable component analysis (dvca): Identifying multiple evoked components using trial-to-trial variability. Submitted, preprint at: www.huginn.com/knuth, 2004.

[2] K. H. Knuth, W.A. Truccolo, S.L.Bressler, and M. Ding. Separation of multiple evoked responses using differential amplitude and latency variability. In T.W. Lee, t.P. Jung, s. Makeig, and T.J. Sejnowski, editors, *Proceedings of the Third International Workshop on Independent Component Analysis and Blind signal Separation: ICA 2001*, 2001.

[3] Robert Plonsey and David G. Fleming. *Bioelectric Phenomena*. McGraw-Hill Book Company, New York, 1969.

[4] Kevin R. Wheeler and Charles C. Jorgensen. Gestures as input: Neuroelectric joysticks and keyboards. *IEEE Pervasive Computing*, 2(2), April-June 2003.

[5] Kevin C. McGill. Optimal resolution of superimposed action potentials. *IEEE Transactions on Biomedical Engineering*, 49(7), July 2002.

[6] Daniel William Stashuk. Decomposition and quantitative analysis of clinical electromyographic signals. *Medical Engineering & Physics*, 21, 1999.

[7] Daniel Zennaro, Peter Wellig, Volker M. Koch, George S. Moschytz, and Thomas Laubli. A software package for the decomposiion of long-term multichannel emg signals using wavelet coefficients. *IEEE Transactions on Biomedical Engineering*, 50(1):58–69, January 2003.

[8] Jianjun Fang, Gyan C. Agarwal, and Bhagwan T. Shahani. Decomposition of multiunit electromyographic signals. *IEEE Transactions on Biomedical Engineering*, 46(6):685 – 697, June 1999.

[9] Dario Farina, Elena Fortunato, and Roberto Merletti. Noninvasive estimation of motor unit conduction velocity distribution using linear electrode arrays. *IEEE Transactions on Biomedical Engineering*, 47(3):380 – 388, March 2000.

[10] Dario Farina and Roberto Merletti. A novel approach for precise simulation of the emg signal detected by surface electrodes. *IEEE Transactions on Biomedical Engineering*, 48(6):637–646, June 2001.

[11] Dario Farina, Luca Mesin, Simone Martina, and Roberto Merletti. A surface emg generation model with multilayer cylindrical description of the volume conductor. *IEEE Transactions on Biomedical Engineering*, 51(3):415–426, March 2004.

[12] Roberto Merletti, Loredana Lo Conte, Elena Avignone, and Piero Guglielminotti. Modeling of surface myoelectric signals - part i: Model implementation. *IEEE Transactions on Biomedical Engineering*, 46(7):810–820, July 1999.

[13] Roberto Merletti, Serge H. Roy, Edward Kupa, Silvestro Roatta, and Angelo Granata. Modeling of surface myoelectric signals - part ii: Model-based signal interpretation. *IEEE Transactions on Biomedical Engineering*, 46(7):821–829, July 1999.

[14] Tadashi Masuda and Tsugutake Sadoyama. Topographical map of innervation zones within single motor units measured with a grid surface electrode. *IEEE Transactions on Biomedical Engineering*, 35(8):623 – 628, August 1988.

[15] Kevin c. McGill, Zoia C. Lateva, and Shaojun Xiao. A model of the muscle action potential for describing the leading edge, terminal wave, and slow afterwave. *IEEE Transactions on Biomedical Engineering*, 48(12):1357 – 1365, December 2001.